Article

Innovative Bio-Vehicle For Resveratrol And Tocopherol Based On Quinoa 11s Globulin. Nanocomplexes Design And Characterization

Alejandra Rubinstein , Guadalupe Garcia Liñares , Valeria Boeris , Oscar Perez *

Posted Date: 15 July 2024

doi: 10.20944/preprints202407.1087.v1

Keywords: 11S globulin; quinoa; bioactive compounds; complexation; aggregation; nutraceutical products; functional ingredient

 doi:10.20944/preprints202407.1087.v1

Article

Innovative Bio-Vehicle For Resveratrol And Tocopherol Based On Quinoa 11s Globulin. Nanocomplexes Design And Characterization

Alejandra J. Rubinstein [1], Guadalupe Garcia Liñares [2], Valeria Boeris [3] and Oscar E. Pérez [1,*]

[1] Consejo Nacional de Investigación Científica y Técnicas de la República Argentina, IQUIBICEN-CONICET. Departamento de Química Biológica, Facultad de Ciencias Exactas y Naturales, Universidad de Buenos Aires. Intendente Güiraldes, s/n, Ciudad Universitaria, Buenos Aires, C1428EGA, Argentina

[2] Laboratorio de Biocatálisis. Departamento de Química Orgánica y UMYMFOR, Facultad de Ciencias Exactas y Naturales, Universidad de Buenos Aires-CONICET, Intendente Güiraldes, s/n Ciudad Universitaria, C1428EGA Buenos Aires, Argentina.

[3] Área Fisicoquímica, Departamento de Química Física, Facultad de Ciencias Bioquímicas y Farmacéuticas, Universidad Nacional de Rosario (UNR)–CONICET, Suipacha 531, Rosario, Argentina

* Correspondence: author: Oscar E. Pérez. Tel: +54 11 45763342; E-mail address: oscarperez@qb.fcen.uba.ar

Abstract: The objective of the present contribution was to design and characterize resveratrol (RSV) and tocopherol (TOC) loaded 11S quinoa seed protein nanocomplexes. Firstly, molecular docking was performed to describe the probable binding sites between protein and ligands. Isothermal titration calorimetry allowed to obtain the thermodynamic parameters that described the molecular interactions between RSV or TOC with the protein. 11S globulin intrinsic fluorescence spectra showed a quenching effect exerted by RSV and TOC, demonstrating protein-bioactive compounds interactions. Stern-Volmer, Scatchard and Förster resonance energy transfer models application confirmed static quenching and allowed to obtain parameters that described the 11S-RSV or 11S-TOC complexation process. Secondly, protein aggregation induced by bioactive compounds interactions was confirmed by dynamic light scattering and atomic force microscopy with diameters <150 nm, detected by both techniques. Finally, it was found that antioxidant capacity of single 11S globulin did not decrease, meanwhile was additive for 11S-RSV. These nanocomplexes could constitute a real platform for the design of nutraceutical products.

Keywords: 11S globulin; quinoa; bioactive compounds; complexation; aggregation; nutraceutical products; functional ingredient

1. Introduction

Quinoa (*Chenopodium quinoa Willd*.) is an ancient crop indigenous from the Andean regions of South America. In recent years, quinoa seeds have gained renewed attention due to their exceptional nutritional properties, including high-value proteins and the presence of antioxidant molecules [1,2]. Quinoa's 11S globulin, also known as chenopodin, represents the most significant seed storage protein with a structure resembling glycinin, the 11S globulin found in soybeans. Quinoa 11S globulin is composed of a basic subunit of 17–20 kDa and an acid subunit of 30–35 kDa interconnected by disulfide bonds [3]. Otherwise, resveratrol (RSV), (3, 5, 4'-trihydroxystilbene), is categorized as a non-flavonoid polyphenol, naturally occurring in both trans and cis isomers. Numerous studies have demonstrated the efficacy of RSV in mitigating a wide range of diseases, including diabetes mellitus, metabolic syndrome, obesity, inflammation, cardiovascular issues, and neurodegenerative conditions [4]. However, RSV has low water solubility and limited bioavailability. Additionally, RSV is highly vulnerable to oxidative conditions, leading to rapid degradation and extensive metabolism. Therefore, the constrained bioavailability underscores the necessity for the development of more suitable RSV formulations to protect its bioactivity[5]. α-Tocopherol (TOC) represents the predominant and biologically active variant of lipophilic vitamin E, known for its capacity to diminish the risk of various chronic diseases linked to oxidative stress. Numerous studies have

 doi:10.20944/preprints202407.1087.v1

demonstrated the potential health benefits associated with the consumption of vitamin E. However, the application of this nutrient is conditioned by its hydrophobic nature and its inherent sensitivity to oxygen, heat, and light. Tocopherols are easily oxidized when exposed to air, especially in the presence of iron [6].

Protein molecules have the capacity to spontaneously link ligands. In this context, previous reports indicate this topic as a strategy to transport bioactive compounds of importance in public health, constituting true functional ingredients[7–12]. Specifically, when a bioactive compound interacts with a protein, a novel structure emerges, the complexes, which could form aggregates via self-assembly. Consequently, self-assembled complexes constitute nanocomplexes when their dimensions fall within the nanoscale [13]. Nanocomplexes, which possess immense potential to function as nanovehicles, can link diverse ligand compounds. One particularly intriguing characteristic of these nanocomplexes is their ability to encapsulate and release preloaded compounds, such as RSV or TOC within a specific environment. The release mechanism of the bioactive compound, the ligand, can be regulated through adjustments in pH levels, temperature, or ionic strength [14].

Various endeavors have been undertaken to create nanovehicles through nanocomplexation systems, enabling the targeted release of biologically significant compounds in pharmaceutical, nutraceutical, and food industries. In this context, the aim of this study was to design and characterize quinoa seeds-11S globulin-based nanocomplexes with RSV or TOC. The underlying idea for this approach is to generate vehicles for RSV and TOC, which can be protected from insulting agents and in turn, the possibility of exerting controlled realize under specific conditions, constituting true functional ingredients for nutraceutical or functional products.

2. Materials and Methods

2.1. Materials

Quinoa (*Chenopodium quinoa Willd.*) defatted quinoa seed flour was obtained from "El Portugues" (seed origin: Peru), with a protein content of 16% db. Protein fraction, with a yield of 60%, was isolated from the defatted quinoa seed flour according to the method proposed by Martinez et al. [11]. Protein determinations were done by Kjedahl method (Nx6.25). TOC and RSV were gently donated by DSM and Temis Lostaló, respectively, both laboratories from Argentina, and used without further purification. Milli-Q water was always used, and all chemicals were of analytical grade.

2.2. 11 S purification

An ÄKTA Protein Purification System, FPLC, was used for quinoa seed 11S globulin purification (GE Healthcare Life Sciences, Germany). It was equipped with Sephadex® S200 10/300 GL (GE Healthcare Life Sciences, Uppsala, Sweden) column. Aliquots of 1 mL containing the total globulins equilibrated for 12 h at 20 °C were submitted to the size exclusion chromatography process. Samples were eluted with distilled water at pH 9, at a flow rate of 0.3 mL/min at 25 °C. Fractions of 1.5 mL were collected and analyzed by absorbance at 280 nm. The eluted fraction corresponding to 11S globulin was stored at −20 °C up to the moment in which they were employed.

2.3. SDS-PAGE electrophoresis

The fraction corresponding to total globulins were analyzed in SDS-PAGE according to Laemmli [15] with a Mini-Protean II device (Bio-Rad, CA, USA). 12% of polyacrylamide running gel was used under denaturing conditions. Runs were performed at 90 V. 40 μg of protein was deposited in each well of the stacking gel. After electrophoresis, a Coomassie brilliant blue staining was performed to detect proteins of interest [16].

2.4. Molecular docking

 doi:10.20944/preprints202407.1087.v1

Molecular docking approach was carried out by using AutoDock vina 1.1.2[17]. Given the absence of a crystal structure for quinoa seed 11S globulin, modeling was performed using the 11S globulin of *Amaranthus hypochondriacus* (pdb: 3qac) as homologous. TOC and RSV conformers were obtained from PubChem (https://pubchem.ncbi.nlm.nih.gov) as sdf files, which were transformed into mol2 using the Avogadro 1.2.0 molecular editor. Blind dockings with fixed receptor of all protein-bioactive pairs were performed, with grids that covered the entire macromolecule. To ensure reproducibility of the results, all dockings were repeated 10 times. The lowest energy pose of each complex was analyzed using the VMD v.1.9.3 (visual molecular dynamics) [18], Ligplot and PLIP programs.

2.5. Preparation of 11S and TOC or RSV mixed systems

Samples of 11S globulin and RSV or TOC were dissolved separately in the appropriate solvent and then diluted into distilled water at pH 9 at room temperature under gentle agitation. The solutions were prepared freshly and centrifuged at 10,000 rpm per 10 minutes. The supernatant was kept at 4 °C for 24 h to achieve the complete hydration of the molecules. Thus, the final protein concentration of mixed systems was kept constant at 0.5%, w/w, meanwhile RSV and TOC concentration ranged 0-6250 μM.

2.6. Circular dichroism (CD)

For these exams, single 11S and 11S-RSV and 11S-TOC mixed systems were diluted up to 0.02% w/w of protein with 10 μM of RSV and 250 μM of TOC respectively. The CD spectrum was obtained by a circular dichroism spectrometer (JASCO J-815 CD spectrometer). The wavelength ranged from 190 nm to 260 nm. The bandwidth was set at 1 nm. The spectra for each single bioactive compound, RSV or TOC, were also carried out, without obtaining significant signals. The percentage of protein secondary structure was calculated using the BestSel deconvolution software.

2.7. Isothermal titration calorimetry (ITC)

An ITC apparatus NanoITC (TA Instruments) was used to characterize, from a thermodynamic point of view, the interactions between quinoa 11S globulin and RSV or TOC. To this end, 11S globulin (36.4 μM), and RSV or TOC (876 μM) solutions were prepared using distilled water at pH 9. In the experiment, 50 μL RSV or TOC solution was gradually injected into 200 μL of 11S solution with the injection volume of 2.5 μL for 20 times. The interval, stirring speed and temperature were set at 300 s, 300 rpm and 25 °C, respectively. To subtract the effect of dilution heat, the hydrophobic compound (RSV or TOC) solution was titrated into distilled water at pH 9 and the result was set as a blank. A series of thermodynamic parameters Gibbs free energy (ΔG), enthalpy change (ΔH), entropy change (ΔS) and including the binding constant (Ka), were analyzed by the Nano Analyze software.

2.8. Steady-state fluorescence measurements

Fluorescence spectra for single 11S globulin and 11S-TOC or 11S-RSV mixed solutions were determined using a Cary Eclipse fluorescence spectrophotometer (ThermoSpectronic AMINCO-Bowman, Series 2, USA), at 25 °C. Protein intrinsic fluorescence emission spectra were recorded from 290 to 400 nm with an excitation wavelength of 280 nm. Thus, RSV solutions with concentrations ranging 0-25 μM and TOC ranging 0-1500 μM, were evaluated in mixed solutions. Bioactive compounds fluorescence was also determined under that wavelength range to discard any possible emission. Intermolecular interactions of 11S and bioactive compounds were evaluated from the fluorescence maximum peak of each emission spectra corresponding to mixed solutions in comparison to single 11S spectrum. The Stern-Volmer model can be employed to examine the relationship between fluorescence intensity and concentration dependence [19]:

$$\frac{F_0}{F} = 1 + k_q * \tau_0 * [BIO] = 1 + K_{SV} * [BIO] \qquad \text{(Eq. 1)}$$

 doi:10.20944/preprints202407.1087.v1

where, *[BIO]* is the concentration of the bioactive compound acting as quencher; *F0* and *F* are the fluorescence emission intensities with and without the quencher, respectively; *kq* is the fluorescence quenching rate constant; τ_0 is the fluorescence lifetime of fluorophore in the absence of quencher; and KSV is the Stern-Volmer quenching constant. A linear plot of F_0/F as a function of *[BIO]* allowed to obtain the *Ksv* values from the slope of the straight line. τ_0 was reported to be equal 2.9 ns for the Trp residues of 11S [11,20].

When small molecules independently bind to a group of identical sites on a macromolecule, the equilibrium between unbound and bound molecules can be described using the equation introduced by Bian [21]:

$$log\ (\frac{F_0-F}{F}) = log\ (K_a) + n * log[BIO] \qquad \text{(Eq. 2)}$$

where, *Ka* and *n* are the apparent binding constant and the number of binding sites per 11S molecule, respectively. From the intercept and slope of *log* $(F_0\text{-}F)/F$ vs *log [BIO]*, the values adopted by *Ka* and *n* can be obtained. The *Ka* value indicates the magnitude of the interaction between protein and ligand. Furthermore, the *n* parameter value indicates the sites of association on the protein molecule[19].

The model described by Scatchard (Equation 3), detailed by Wei et al.[22] was an alternative mathematical approach used here to analyze the binding phenomena between 11S globulin and TOC or RSV from the fluorescence experimental data.

$$[11S] * (1 - f_i) = \frac{[BIO]}{n*\left(\frac{1}{f_i}-1\right)} - \frac{1}{n*K_s} \qquad \text{(Eq. 3a)}$$

$$f_i = \frac{f_{li}-f_{lo}}{f_{lmax}-f_{lo}} \qquad \text{(Eq. 3b)}$$

where, *fli* is the maximal intensity in each measured point, *flo* is the maximal intensity without quencher and *fl max* is the maximal intensity with the highest concentration of quencher; *[11S]* is the protein concentration, *[BIO]* is the bioactive compound concentration; *Ks* and *n* are the apparent binding constant and the number of binding sites per 11S molecule respectively.

2.9. Encapsulation efficiency

The amount of RSV or TOC bound to 11S globulin was determined by the difference between the concentration of bioactive compound initially added to the mixed solutions (BIO_N) minus the bioactive compound not bound or free (BIO_S)[12]. This further refers to the amount of RSV or TOC in the supernatant after ultracentrifugation and filtration through a 10 kDa cut off unit (Vivaspin Turbo 15, Sartorius). 5 mL of each sample, 11S – TOC or 11S - RSV 0.1% in distilled water at pH 9 were centrifuged into the filters. Bioactive compound solution was used as a control to determine any loss due to binding to the filter unit. Filters were centrifuged at 4500 ×g for 15 min at 24 °C. The flow through was collected and RSV or TOC concentration determined. For RSV, absorbance at 306 nm was measured at 25 ± 1 °C on a Jasco spectrophotometer. TOC was measured according to Demirkaya and Kadioglu [23] method with an Agilent 7820A chromatographer equipped with a FID detector and G4513A autosampler. Then, EE (%) of RSV and TOC for 11S globulin inspired complexes was determined as:

$$EE(\%) = \frac{BIO_N - BIO_S}{BIO_N} * 100 \qquad \text{(Eq.4)}$$

2.10. Particle Size and ζ-Potential Determinations

Dynamic light scattering (DLS) experiments were conducted using a Horiba Scientific nanoPartica Z-100 apparatus. The measurements were carried out at 25 °C. Samples were contained in a Hellma quartz glass cuvette. The analysis of intensity fluctuations provided the diffusion coefficient of the particles, allowing determination of particle size through the Stokes-Einstein equation. The interpretation of results followed the approach outlined in Perez et al. [14]. For the DLS

 doi:10.20944/preprints202407.1087.v1

analysis, concentrations of RSV in mixed solutions ranged from 10 to 50 μM, while TOC concentration ranged from 250 to 1500 μM.

Additionally, ζ–potential measurements were performed using the same DLS instrument. Samples were contained in semi-disposable Carbon cells. The ζ–potential was derived from the electrophoretic mobility of the particles, and the conversion of this data into ζ–potential was accomplished using Henry's equation.

2.11. Atomic Force Microscopy (AFM)

The methodology used by Carpineti et al.[24] was followed. Briefly, 5 μL of each suspension, 0.05 % w/w, were put to a freshly cleaved muscovite mica. Images were taken in atmosphere dried under a gentle stream of filtered, dry nitrogen. The cantilever used was an MPP-11100 from NanoDevices with a length of 125 micrometers and an elastic constant of 40 N/m, a resonance frequency of 300 Khz, and a tip radius of 8 nm. All images that are shown were analyzed by tapping mode in air. Nanoscope Software was used to process the images by flattening to remove background slope. Experiments were carried out in a temperature-controlled room at 20 ± 1°C, with acoustic hood isolation and active vibration damping.

2.12. Antioxidant Activity of 11S-RSV or 11S-TOC Complexes

2.12.1. ABTS Assay

The antioxidant capacity of 11S-RSV or 11S-TOC nanocomplexes was assessed through the ABTS assay, as outlined in Martinez et al.[11]. In this method, the pre-formed radical monocation of 2,2-azinobis-(3-ethylbenzothiazoline-6-sulfonic acid) (ABTS•+), obtained by oxidizing ABTS with potassium persulfate, serves as a marker. To initiate the process, ABTS was dissolved in water to achieve a final concentration of 7 mM. The ABTS•+ radical cation was generated by reacting the ABTS stock solution with a final concentration of potassium persulfate of 2.45 mM. The mixture was allowed to stand in darkness at room temperature for 12–16 hours before use. The assessment of antioxidant activity for 11S-RSV or 11S-TOC nanocomplexes was conducted after diluting the ABTS•+ solution with phosphate buffer to achieve an absorbance of 0.80–0.90 (A_0) at 734 nm. Next, 2.5 mL of this solution was mixed with 0.5 mL of sample and the absorbance decrease (*Ainf*). Therefore, ABTS•+ scavenging capacity was calculated as:

$$\text{ABTS}^{\bullet+}\text{ scavenging capacity (\%)} = \left(\frac{A_0 - A_{inf}}{A_0}\right) \times 100 \qquad \text{(Eq. 5)}$$

2.12.2. Ferric reducing antioxidant power (FRAP) assay.

The FRAP assay was executed following the methodology outlined by Martinez et al.[11]. Aliquots of 40 μL of 11S, RSV, TOC, 11S-RSV, or 11S-TOC nanocomplexes, along with the standard solution of GA were dispensed into a test tube containing 600 μL of the FRAP reagent solution. The mixture was then kept in the dark at 25 °C for 30 minutes and the absorbance was measured at 593 nm.

2.13. Statistical analysis

All experiments were performed at least in triplicate. Results were expressed as mean ± SD. The model's goodness-of-fit was evaluated by the coefficient of determination (R^2) using GraphPad Prism 8.0. software.

3. Results

3.1. SDS-PAGE- FPLC

Size exclusion chromatography was used to obtain the quinoa 11S globulin fraction. Chromatograms obtained firstly revealed a peak corresponding to a high molecular weight (MW)

 doi:10.20944/preprints202407.1087.v1

protein fraction and other peaks corresponding to smaller polypeptides (Figure 1 A). The chromatogram pattern presented several populations as others previously reported protein extracts such as quinoa, wheat, and whey [11,25,26]. After that, to analyze the identity of the highest MW protein, SDS-PAGE were performed. The molar mass of the major protein band was around 55 kDa, corresponding to 11S. Due to the presence of disulfide bridges connecting the acidic and basic subunits of quinoa 11S globulin, it is anticipated that, under non-reducing conditions, the subunits will migrate together (Figure 1.B lane B), whereas in the presence of β-mercaptoethanol, 11S subunits will migrate separately (Figure 1.B, lane A)[27]. Under non-reducing conditions, electrophoresis revealed the typical pattern of 11S globulin with acidic and/or basic subunits at 30–35 kDa and 17–20 kDa respectively (Lane A). This pattern was already found by Brinegar and Goundan [28], who presented the first report concerning to 11S globulin from quinoa purification. Furthermore, this pattern was also found for 11S globulins of other seeds such as amaranth or soybeans. In this regard, Abugoch et al.[29] studied amaranth proteins isolation and found the 11S globulin fraction consisting of 2 subunits with approximately 20 and 30 kDa, respectively.

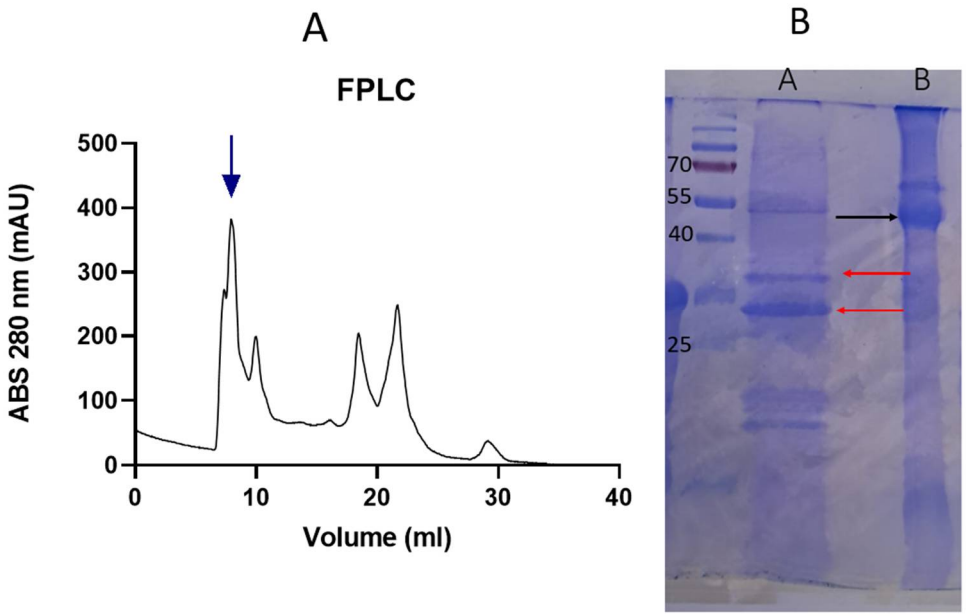

Figure 1. A- Elution profile by FPLC of quinoa protein extract. B-SDS-PAGE. Lane A: quinoa extract under reducing conditions. Red arrows: 11S basic and acid subunits- Lane B: Quinoa extract under non-reducing conditions. Black arrow: 11S (numbers indicate the MW of markers).

3.2. Molecular Docking

Bioinformatics tools are useful for predicting the binding site and energy between a protein and a ligand, in this case the approach was used for quinoa 11S globulin with TOC or RSV. Docking is widely used to compare binding energies between different ligands or different proteins [9,30,31]. The pose with the lowest energy of TOC molecule into the quinoa 11S crystals is presented in Figure 2A. It is observed that the TOC bound and fit in the hydrophobic pocket formed by the amino acids LEU85, LEU87, PRO88, HIS142, GLN143, TRP163, LYS248, VAL260 with a binding energy of -6.22 kcal/mol. This energy was the result of the formation of a hydrogen bond between the carbonyl oxygen of TOC molecule and the amino acid TRP163, a salt bridge and several hydrophobic interactions as can be seen in Table 1.

Table 1. Parameters derived from molecular docking analysis of 11S-TOC and 11S-RSV mixed-systems.

 doi:10.20944/preprints202407.1087.v1

Complex	Binding energy (kcal/mol)	Hydrogen Bonds	Hydrophobic interactions	Saline bridge	Total
11S-RSV	-5,64	4	4	0	8
11S-TOC	-6,22	1	10	1	12

Docking was also performed between quinoa 11S globulin and RSV. The lowest energy pose for RSV in the 11S crystals is shown in Figure 2B. It is observed that RSV bound the helices determined by the amino acids ALA427, ILE433 and ARG459 with a binding energy of -5.64 kcal/mol. This energy was the result of the formation of hydrogen bonds with the amino acids GLY428, TYR445 and ARG459, to which also contribute several hydrophobic interactions as seen in Table 1. The values of binding energy were very similar, without showing statistical differences between both bioactive compounds.

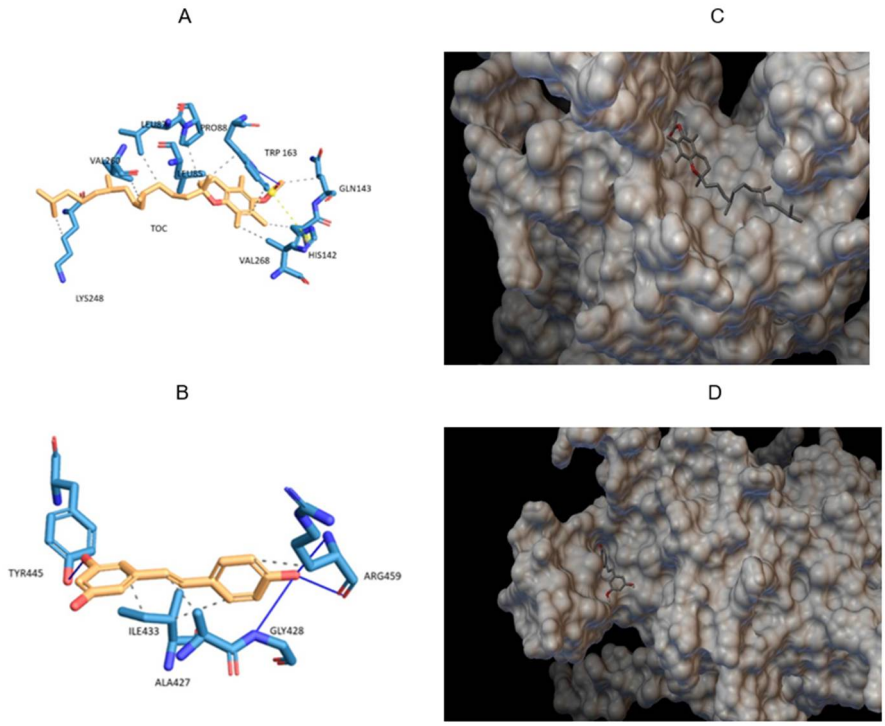

Figure 2. Lower energy poses for the systems consisting of TOC (A) or RSV (B), pointing out the amino acid residues involved in the binding with the analyzed bioactive compounds; and the crystalline structure of 11S-RSV (C) and 11S-TOC (D), obtained by molecular docking.

3.3. Circular Dichroism (CD)

To elucidate any changes induced by the bioactive compounds on the secondary structure of the 11S globulin, CD spectroscopy of the 11S-RSV and the 11S-TOC mixtures were determined. In general terms, the CD spectrum of 11S had a broad negative peak at 205 nm (Figure 3A). When the bioactive compounds were added, some changes were observed in the CD spectra of 11S, suggesting that the bioactive compounds altered the protein secondary structure, as explained by Liu et al. [10]. Specifically, Figure 3B showed that the secondary structure composition of single 11S globulin were 1.8 % α-helix, 46% β-sheet, 15.9% β-turn and 36.3% other disordered patterns. When the RSV was added, the contents of α-helix, β-sheet and β-turn were decreased to 0%, 41.6% and 14.7%, respectively, while the contents of other patterns were increased to 43.7%. When TOC was present in the system, the contents of α-helix, β-sheet and β-turn also decreased. In fact, for TOC the CD peak shifted from 205 to 201 nm, suggesting that the conformation of 11S globulin was transited from disorder to order [10].

 doi:10.20944/preprints202407.1087.v1

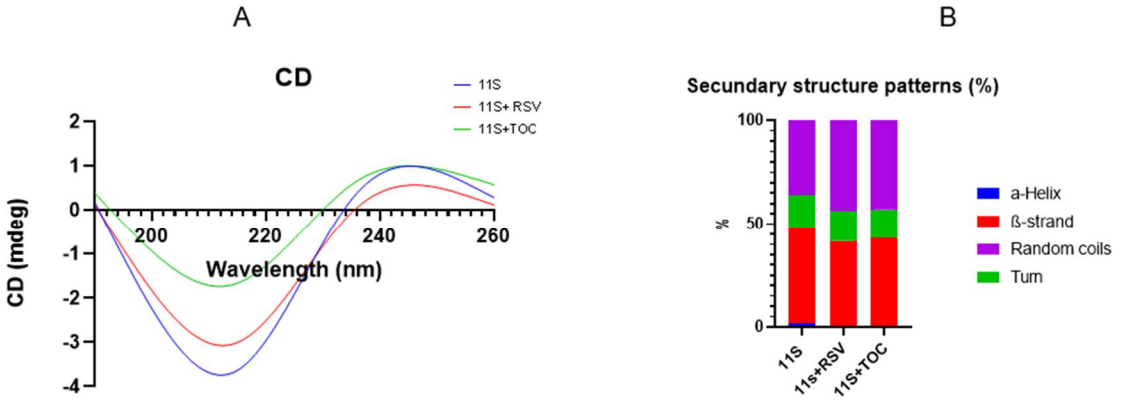

Figure 3. A) Circular dichroism spectra and B) Secondary structure fractions, for 11S globulin and for 11S-RSV and 11S-TOC mixed systems.

3.4. Isothermal Titration Calorimetry (ITC)

The interaction between 11S and RSV or TOC was further deepened by ITC. As shown in Figure 4 and Table 2, $\Delta G < 0$ and $\Delta H < 0$ and, indicating the bindings of 11S and TOC or RSV were spontaneous and exothermic respectively. Moreover, the intensity of the peaks gradually decreased with the increase of bioactive compound concentration. These results suggested that 11S globulin was gradually saturated, or in other words, the binding sites tended to be saturated[10]. In addition, the 11S-RSV had a greater Ka value than 11S-TOC (Table 2). Moreover, the Ka value for 11S-RSV resulted one order greater than for 11S-TOC. This phenomenon would indicate that RSV and 11S globulin had the strongest binding ability, which means that RSV would be more prone to form complexes with this protein.

Table 2. Binding sites (n), binding constant (KA), dissociation constant (Kd), enthalpy change (ΔH), entropy change (ΔS) and ΔG (Gibbs free energy) for the interaction between TOC or RSV and 11S.

Bioactive compound	*n*	K_d(μM)	K_a(M^{-1})	ΔH(kJ/mol)	ΔS(J/K*mol)	ΔG(kJ/mol)
TOC	0.85 ± 0.03	340 ± 40	(2.9 ± 0.8) * 10^3	-45 ± 2	100 ± 10	-20 ± 1
RSV	0.91 ± 0.04	48.2 ± 1	(2.1 ± 0.3) * 10^4	-43 ± 7	-63 ± 5	-24.6 ± 0.2

 doi:10.20944/preprints202407.1087.v1

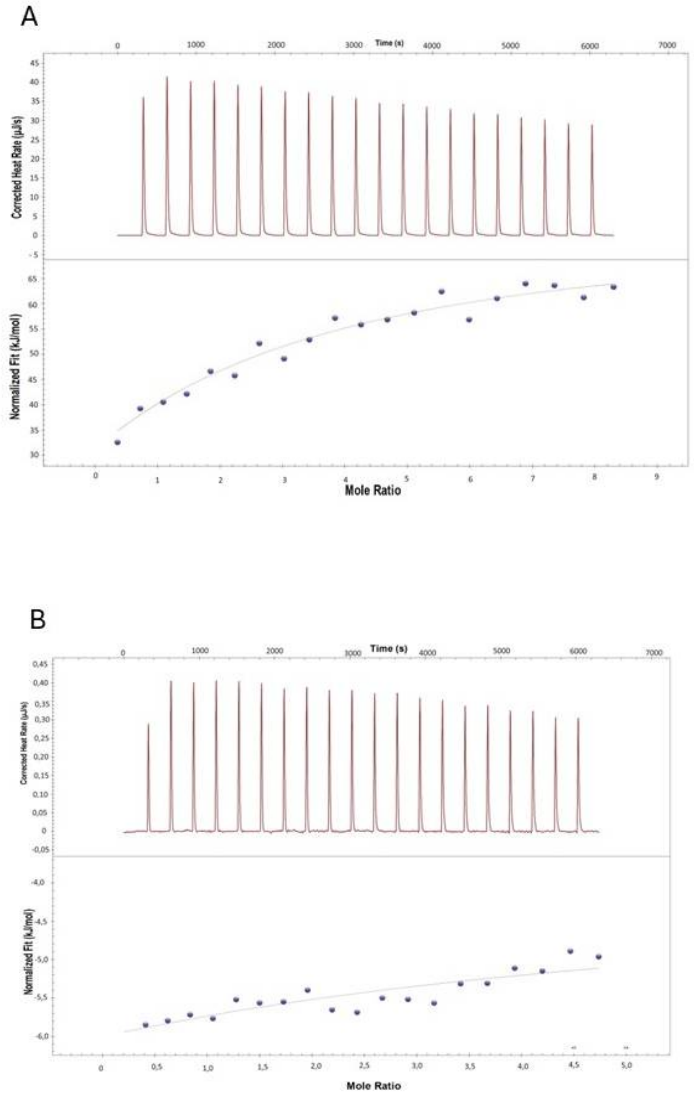

Figure 4. Experimental calorimetric data associated with ITC determinations at 298 K concerning to the interactions of 11S with bioactive compounds RSV (A) and TOC (B) respectively.

3.5. Fluorescence Spectroscopy

Fluorescence spectroscopy is a suitable method for assessing ligand-protein interactions [7,12]. In this context, 11S-TOC and 11S-RSV interactions were evaluated from their respective fluorescence emission spectra of mixed system. Figure 5 shows the emission spectra for the mixed 11S-TOC and 11S-RSV mixed solutions with different bioactive compound concentrations, in comparison with that of the single protein. The maximum fluorescence intensity value was 8.13. When both bioactive compounds were added, results evidenced that the fluorescence intensity decreased as the TOC or RSV concentration increased in the respective bulk solution. The results on intrinsic protein fluorescence quenching, confirm the existence of protein-ligand interactions. To elucidate the type of quenching existing between 11S protein and RSV or TOC, the Stern-Volmer and the Scatchard models were applied.

These models were previously used by diverse authors to study the interaction between different proteins and bioactive compounds [7]; [32]; [33]. S. Figure 1 shows the dependence of F_0/F and RSV or TOC concentration. The value of Ks, the affinity constant, could be obtained from the slope of the curve (Table 3).

 doi:10.20944/preprints202407.1087.v1

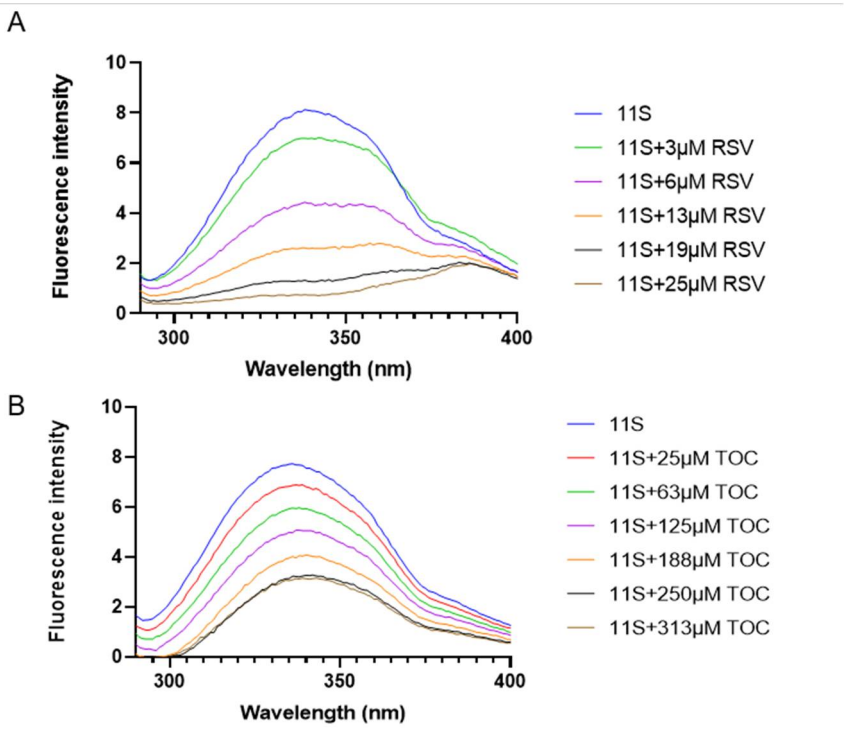

Figure 5. Fluorescence emission spectra of quinoa 11S globulin 0.1%, w/w, in the presence of various concentrations of RSV (A) or TOC (.B)

When small molecules have the potential to bind independently to a set of equivalent sites on a macromolecule, the equilibrium between free and bound molecules is given by Equation 2. This expression allowed to analyze the dependence of fluorescence intensity with RSV or TOC concentration for static quenching [12]. From the plot log [(F0- F)/F] vs log [BIO] (Stern Volmer model) the *n* value can be obtained which relates the number of binding sites on the protein molecule. For Stern Volmer model, *n* resulted 1.04 and 2.35 for mixed systems with RSV and TOC, respectively.

Table 3. Fluorescence modeling parameters derived from the application of Stern-Volmer, Scatchard and FRET.

	TOC	RSV
Stern-Volmer model		
Ksv (M^{-1})	4800	385700
Kq (M^{-1} s^{-1})	$1.66*10^{12}$	$1.13*10^{14}$
n	1.04	2.35
R^2	0.9931	0.9406
Scatchard model		
K (M^{-1})	151478	3852674
n	8.87	0.90
R^2	0.9422	0.9707
Förster resonance energy transfer (FRET)		
J (λ) (cm3/M)	$1.14*10^{13}$	$2.67*10^{13}$
R0 (nm)	5.39	6.22

Preprints.org (www.preprints.org) | NOT PEER-REVIEWED | Posted: 15 July 2024 doi:10.20944/preprints202407.1087.v1

Employing Scatchard model, we obtained Ks value of $1.5*10^5$ M^{-1} for TOC and $3.8*10^6$ M^{-1} for RSV, respectively (Table 3). These values manifested the trend observed with Stern-Volmer model: the binding force of 11S and RSV was one order of magnitude higher than for 11S and TOC. According to the Scatchard model, the parameter *n* resulted equal to 8.87 and 0.9 for mixed systems with TOC and RSV, respectively (Table 3). The calculated binding sites can result different when different models are considered as previously reported[11]. Concerning to this, Wei et al. [22] in a very interesting and useful contribution, asserted that researchers could obtain different binding parameters with different mathematical models. So, it is difficult to evaluate which model is more appropriate. This author also obtains different *n* values with the different models applied to the fluorescence data obtained from BSA - RSV mixed systems.

Since fluorescence quenching of 11S by TOC or RSV may have an additional contribution due to Förster resonance energy transfer (FRET), the extension of such phenomenon was also studied for the whole range of RSV and TOC concentrations. The fluorescence spectrum of 11S globulin and the absorbance spectrum (λex = 280 nm and λem= 290-400 nm) of TOC and RSV were overlapped (Figure 6) and the distance (r) between molecules were determined as proposed by Chilom et al. [34].

$$E = 1 - \frac{F}{F_0} = \frac{R_0^6}{R_0^6 + r^6} \qquad \text{(Eq. 6)}$$

where E is the efficiency of energy transfer, F_0 and F are the same parameters previously described, *r* is the distance between acceptor and donor, and R_0 is the critical distance when the energy transfer efficiency is 50 %, and it was calculated as:

$$R_0^6 = 8.79 * 10^{-5} * K^2 * N^{-4} * \phi * J(\lambda) \qquad \text{(Eq. 7)}$$

being K^2 the spatial orientation factor of the donor, N the refractive index of the medium, Φ the fluorescence quantum yield of the donor, and J(λ) the overlap integral of the absorption spectrum of the acceptor and the fluorescence emission spectrum of the donor. J(λ) was calculated with the Fluortools software (Table 3). Using K^2 = 2/3, n = 1.336, and Φ = 0.118 [34], the critical distance R_0 = 5.39 nm and 6.22 nm was calculated for TOC and RSV respectively. Bustos et al. [7] reported different R_0 value 3.07 nm for BSA–folic acid mixed system, which might be explained considering the different nature and intrinsic characteristics of this protein-ligand pair. Additionally, the distance *r* between 11S globulin and TOC or RSV and the efficiency of energy transfer E were determined for each bioactive compound using Eq. (6). As shown in Supplementary Figure 2, the *r* values decreased from 7.79 to 5.09 nm as the TOC concentration varied between 250 and 313 µM. Meanwhile for RSV, the r values decreased from 15.54 to 4.24 nm conform the RSV concentration varied between 1 and 25 µM in the mixed system.

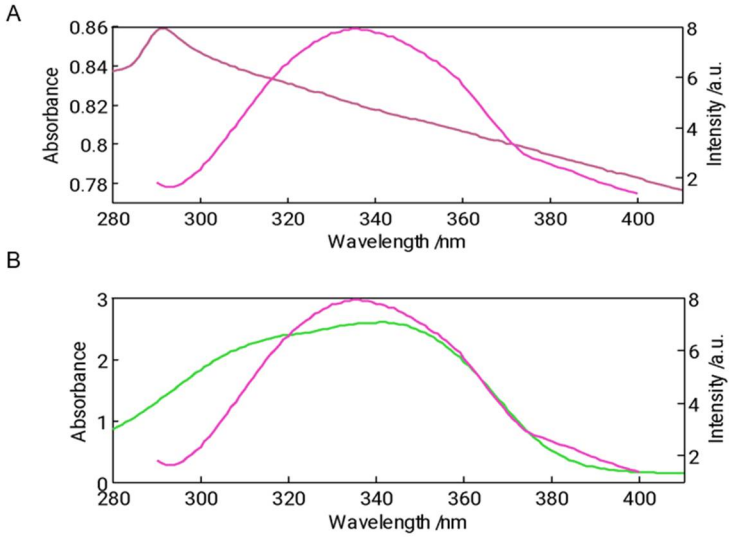

Figure 6. Overlapping between fluorescence emission spectrum of (A) 11S and UV absorption spectrum of TOC and (B) 11S and UV absorption spectrum of RSV. Both at λex= 280 nm.

 doi:10.20944/preprints202407.1087.v1

3.6. EE determination

The EE of 11S globulin resulted in the order of 37 and 73%, for RSV and TOC, respectively. These results resulted higher than those found by Martinez et al. [11], who used the purified quinoa 11S globulin for commercial betanin encapsulation, obtaining an EE of 23%.

3.7. Analysis of 11S globulin aggregation induced by RSV or TOC

Particle size distribution for 11S and 11S-RSV or 11S-TOC mixed solutions were obtained by DLS. This analysis enables understanding the aggregation process of various proteins, with the aim of either preventing it or leveraging it for specific applications [12]. Numerous investigations have indicated that protein unfolding, and aggregation may take place, influenced by factors such as protein composition/concentration, pH, ionic strength, ion concentration, fat content, and other variables [35]. Thus, focus was put on the possible 11S aggregation induced by RSV or TOC addition as this phenomenon could be concurrent with complexation with ligands [36].

Intensity vs particle size distribution revealed the presence of one population in all cases analyzed (Figure 7A and 7B). When analyzing the single 11S globulin protein distribution, a single population centered at 31 nm was found. 11S- RSV mixed systems showed an increase in particle size as the concentration of this bioactive increased. At the maximum concentration, a particle reached a mean of 60 nm for the particle size distribution, doubling the size obtained for the protein alone solutions.

 doi:10.20944/preprints202407.1087.v1

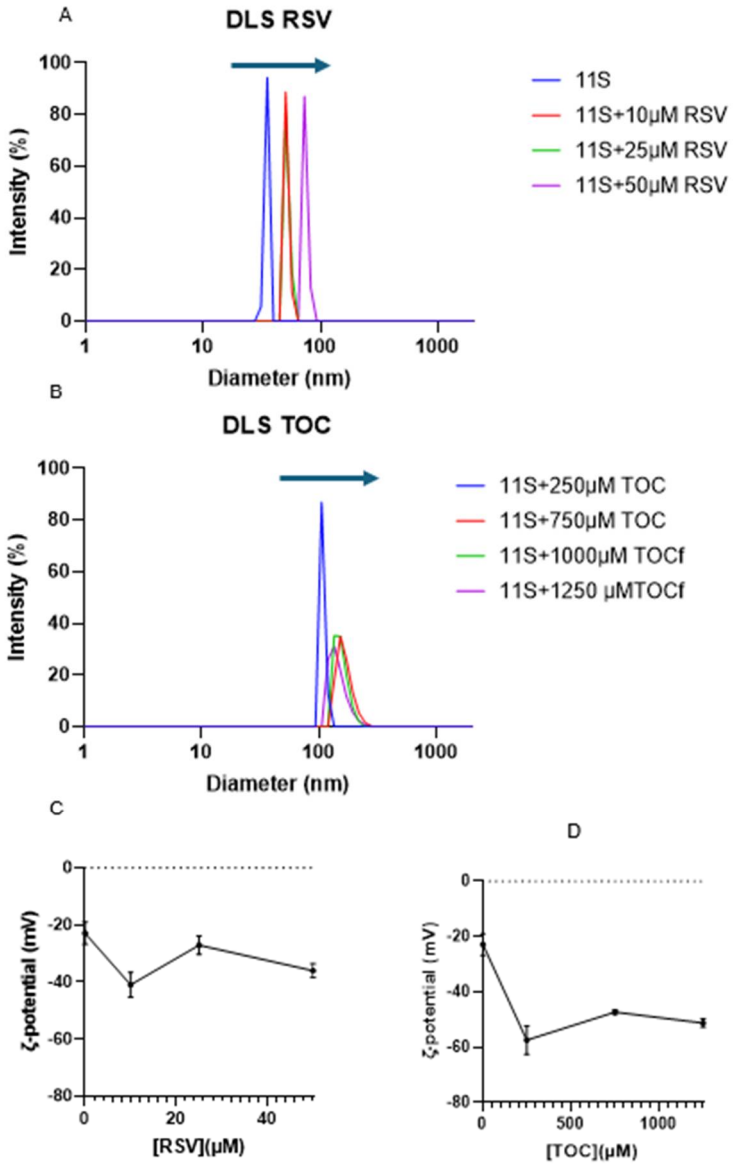

Figure 7. Particle size distribution for 11S-RSV(A) and 11S-TOC (B) expressed in intensity. Arrows indicate the displacement of the global distribution to higher sizes. Variation of ζ-potential for 11S-RSV (C) and for 11S-TOC (D), where each point represents the mean±SD, n=3.

Likewise, when TOC was added an increase in particle size was also observed. In fact, for the two highest concentrations of TOC (1000 and 1250 µM) the particle size could not be measured as the aggregation induced by this bioactive was extensive and the dimensions of the entities generated exceeded the detection limits of the device. For this reason, it was necessary to filter the samples with a 0.45 µm filter samples could be read with the equipment confirming that large aggregates were generated by adding these concentrations of TOC.

ζ-potential emerges as a critical parameter for characterizing nanovehicles, with broad potential applications in industries such as pharma, food, nutraceuticals, and cosmetics. Analysis of ζ-potential measurements revealed that 11S exhibited values of −23 mV (Figure 7 C and D). After any bioactive compound addition, an increase in the modulus of ζ-potential was observed, which indicates an increase in the stability of the mixtures.

3.8. Atomic force microscopy (AFM)

 doi:10.20944/preprints202407.1087.v1

The study food biopolymers by AFM can be roughly categorized into providing new data on commonly used materials, exploring structure–function relation, and the characterization of newly isolated/synthesized materials [37]. However, only one report was found on the aspects of 11S quinoa-based aggregates using AFM, at least using the most common search engines, which describes the disaggregation induced by of high intensity ultrasound application on 11S quinoa aggregates [38]. AFM images are shown in Figure 8, where the analysis for the considered samples is presented as: Column I, showing the picture with topographical aspect obtained by the AFM technique; Column II shows the length between the maximum and minimum height possible and Column III describes the height and also the full width taken at half maximum diameter as determined through cross-sectional analysis of the width of the image (1000 nm). When taking images of the purified single 11S globulin, particles with an average diameter of 45 nm were observed, i.e. sizes falling into the nanoscale. RSV and TOC addition also seemed to contribute to a particle size increase, making detectable nanostructures of 100 nm in both cases. This is the confirmation that 11S-RSV and 11S-TOC complexes constituted entities that fell on the nanoscale.

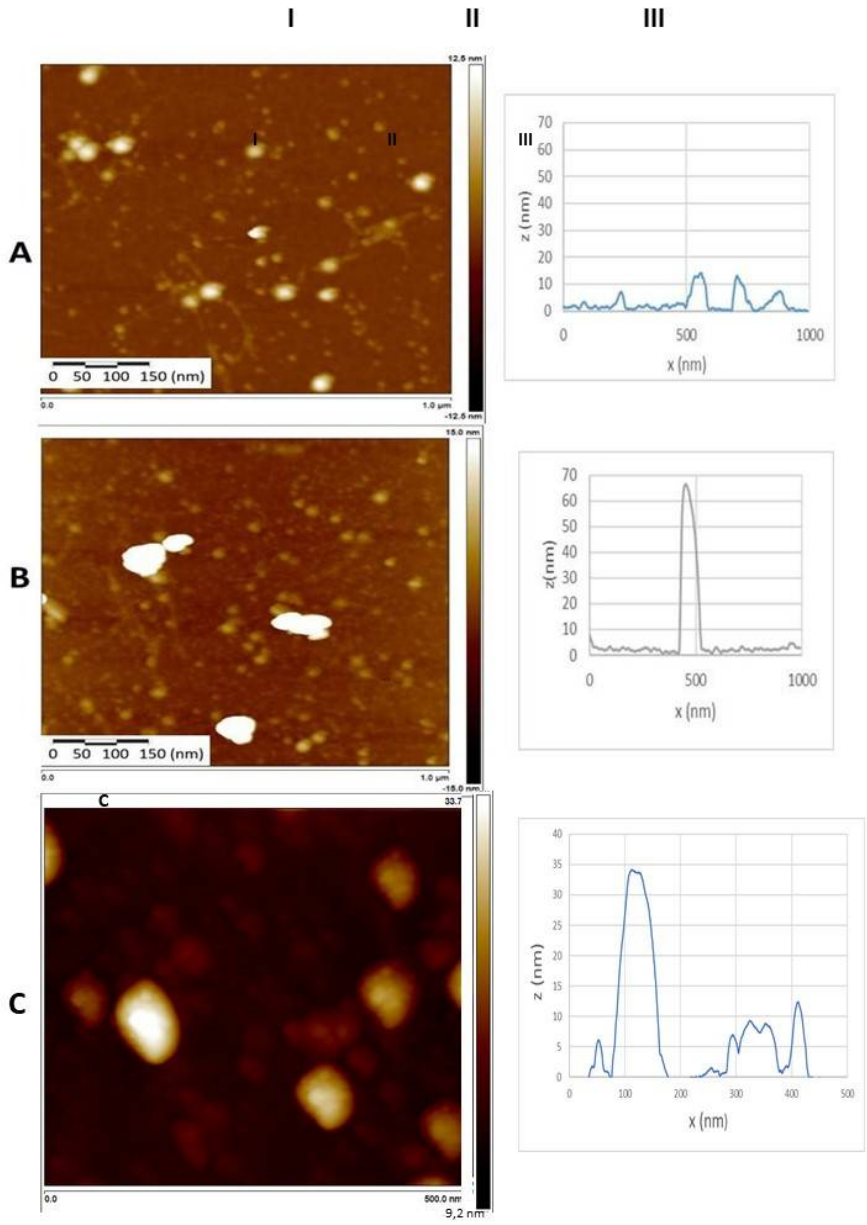

Figure 8. AFM imaging for: A) single 11S globulin; B) 11S+RSV; and C) 11S+TOC mixed systems.

 doi:10.20944/preprints202407.1087.v1

3.9. Antioxidant capacity of 11S-RSV and 11S-TOC nanocomplexes

3.9.1. ABTS

The ABTS method was used to evaluate the antioxidant capacity of 11S quinoa protein and its mixtures with different concentrations of TOC or RSV (Figure 9A and 9B, respectively). The protein presented antioxidant capacity by its own, for instance, a 11S concentration of 0.1%, demonstrated an antioxidant activity of 59 ± 6 %. This property was previously reported by Martinez et al. [11] and it was attributed to the presence of specific amino acids such as Trp, Tyr and Met, which have the highest antioxidant activity. followers of Cys, His and Phe. The antioxidant activity of these amino acids can be explained in terms of their ability to donate hydrogen atoms; Cys can also donate thiol groups [39]. Regarding to RSV, as the concentration of this bioactive increased, the antioxidant capacity also increased. It is well known the RSV antioxidant capacity. For example, Gülçin [40] used a concentration of 10 µg/ml (43µM) of RSV and achieved practically a total decrease in absorbance in the ABTS assay. Concerning to TOC, this vitamin did not show antioxidant capacity as the bioactive used was in the form of tocopherol acetate. With respect to the mixed systems, the scavenging capacity was equivalent to that of protein alone. This means that the complexing process did not decrease the scavenging capacity of the 11S globulin, which is important.

3.9.2. FRAP

In addition to its anti-radical properties, the antioxidant capability of a bioactive compound can be assessed by its reducing power. This power helps to prevent harmful oxidative reactions by creating a reducing environment. To fully quantified the antioxidant capacity of the produced 11S-RSV or 11S-TOC nanocomplexes via FRAP assay was also evaluated. Firstly, a calibration curve was constructed with standard solutions of gallic acid. Then mixtures were made with different concentrations of 11S and RSV or TOC. It can be in Figure 9C and 9D that at null protein concentration, TOC had greater antioxidant capacity at 750 and 1250 µM. With respect to RSV, the same trend as with ABTS was observed: higher concentrations of RSV correlated with greater antioxidant capacity. Also, 11S globulin has antioxidant capacity by its own. Concerning to this, Escribano et al., [41] also found a great antioxidant capacity for different varieties of quinoa grains by applying the FRAP assay.

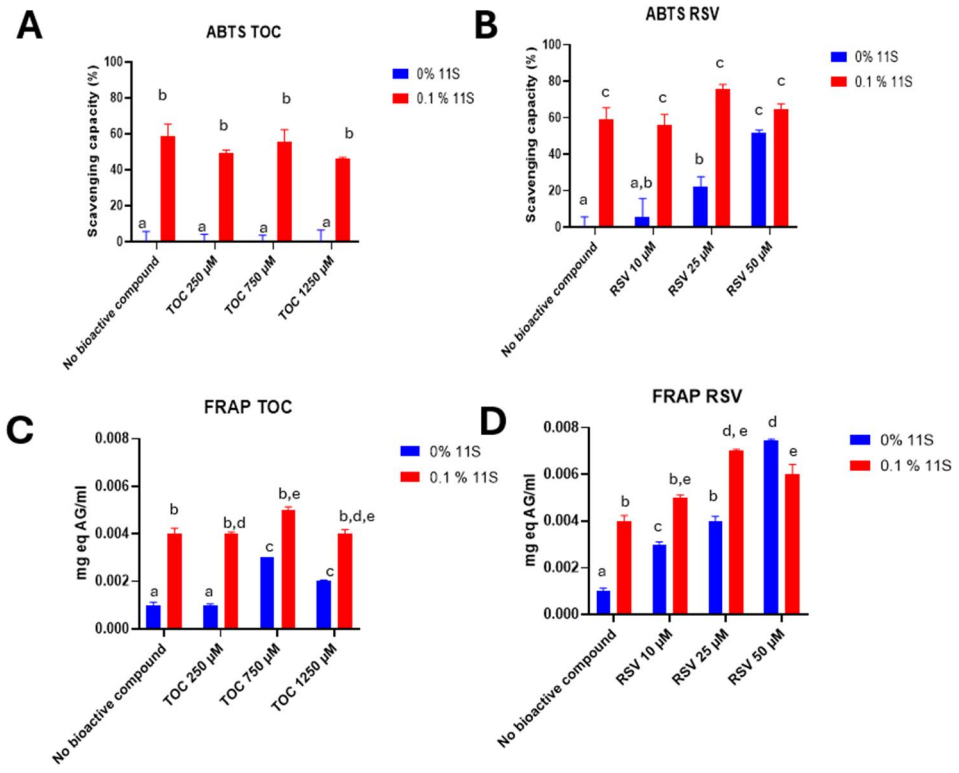

 doi:10.20944/preprints202407.1087.v1

Figure 9. Antioxidant capacity for different concentrations of 11S evaluated by ABTS in TOC (A) and RSV (B) or, FRAP in TOC(C) or RSV (D) mixed systems. Results are expressed as mean±SD, n=3 ($p<0.05$) Means with the same letter represent non-significant differences ($p<0.05$).

4. Discussion

In line, Zhang et al.[42] performed molecular docking between pea 11S protein and the bioactive compounds curcumin, quercetin, and RSV. These authors found binding energies of -5.64, -5.85 and -5.85 kcal/mol, respectively. In this case, RSV bound into a pocket close to TYR161. In this sense, one can see that the docking approach allowed to predict the 11S -RSV or 11S – TOC complexes formation under specific conditions and the points contact on the protein molecule. On the other hand, Chamizo-Gonzalez et al. [43], applying molecular coupling between grape 11S protein and the wine anthocyanin (malvidin 3-O-glucoside), found slightly higher interaction energies than ours which resulted -7.6 and -8.1 kcal/mol. Patnode et al. [44] also practiced molecular docking between the soy 11S globulin and glycerol, sorbitol, or cellulose, finding affinity energies of -4.3, -5.5 and -7.1 kcal/mol, respectively.

According to Chen et al. [45], it can be thought that the modifications in the 11S secondary structure proportions were ascribed to the hydrogen bonding and hydrophobic interaction between 11S globulin and the bioactive compounds, in agreement with the results of interactions predicted by the docking approach. These molecular interactions strengths between 11S globulin and the bioactive molecules, could induce the partial unfolding and intramolecular reorganization of the protein, leading to the variation of its secondary structure [46].

On the other side, Li and Ni [47] performed ITC for the binding of TOC with trypsin and pepsin. The enthalpy values obtained were -11.37 and -13.78 kJ/mol, respectively, which resulted to be in the same order than that found here for 11S globulin and TOC. Additionally, the Ka was also in the same order (10^3 M) and the n was close to 1. The value of the stoichiometric binding number (n) suggests the number of molecules of TOC or RSV combined with one molecule of 11S globulin [47]. Wan et al. [48] worked with 11S of soybeans and found Ka values of the same order (10^3 M). They consider that a Ka value greater than 10^4 M would be indicative of high affinity, so the Ka values obtained by Wan et al. [48] and for 11S-TOC in this contribution suggest non-specific interactions. Concerning to entropy, the positive value obtained indicates that the interactions had an important entropic component and in general, with predominant hydrophobic interactions, which coincides with what was obtained by the docking analysis for 11S and TOC. On the other hand, the negative ΔS for the 11S-RSV mixed system would imply that the binding is driven by the negative enthalpy.

The Kq values were much larger than the maximum admitted for dynamic quenching, which is $1.27*10^{10}$ $M^{-1}s^{-1}$[49]. These results evidence that the fluorescence intensity changed for 11S after TOC or RSV addition and the effect could be attributed to static quenching, i.e. 11S-RSV and 11S-TOC complexes formation. The apparent binding constant Ks was also useful to evaluate the magnitude of molecular interactions. The values revealed a strong binding force between 11S and RSV, which was one order of magnitude higher than for 11S and TOC. Such a result means that the protein manifested a higher affinity for RSV. This result followed the same trend that the results obtained by ITC.

It is interesting to note that the affinity constants obtained through ITC and fluorescence measurements exhibit different values. This discrepancy arises because the measurement principles of both techniques are distinct. In ITC, the constants are derived from thermodynamic equilibria, whereas in fluorescence, the obtained values result from quenching caused by the masking of fluorescent residues due to interaction with the ligand, photochemical approach.

Regarding FRET analysis, Jiang et al. [50] carried out this analysis between BSA and RSV, finding a r value of 3.47 nm and R_0 of 2.71 nm, which are lower than those obtained in this work for 11S. These values resulted much smaller than 7 nm, a criterion value for energy-transfer to occur, i. e. the energy transfer from BSA to trans-resveratrol could occur with a high probability. Therefore, for the 11S globulin, the energy transfer would occur for concentrations greater than 125 μM and 6 μM for TOC and RSV.

 doi:10.20944/preprints202407.1087.v1

Concerning to EE and just for comparison, Li et al. [51] designed encapsulating nanoparticles based on a novel construct prepared via Maillard reaction between a soy protein isolate (SPI) and a polyguluronate, an acidic homopolymer of α-(1,4)-L-guluronate separated from alginate, finding RSV EE of 86.66 %. Khan et al. [52] worked with Kafirin, a prolamin type protein obtained from sorghum, and was combined with β-lactoglobulin (β-lg) and casein (CAS) for generating nanoparticles via anti-solvent precipitation method. These entities were used for RSV entrapment giving an EE of around 73 and 69% for kafirin/CAS and kafirin/β-lg at the maximum RSV concentration used. The ability of pea protein isolates (PPI) to form complex coacervates with different gums (Arabic, tragacanth and tara) was evaluated for the encapsulation of α-TOC by Carpentier et al. [53]. The performance of the complex coacervates was studied according to the protein/polysaccharide mixture and protein/polysaccharide ratio. These authors informed a maximum EE of about 77.4% for the coacervates in comparison with the 53.4% obtained for single PPI. Besides, Xu et al. [54] developed O/W emulsions with 5% of oil phase and using whey protein isolate-chitosan complexes as emulsifiers agent for α-TOC encapsulation, at pH 5.7, getting EE of 86.2%.

The works cited above demonstrate the diversity and complexity of the encapsulation platforms used for RSV and TOC. Then, it is clear that the EE is highly dependent on the encapsulation platform used. However, in this contribution EE values obtained for TOC using a single isolated globulin, was in the order of those reported in the literature.

When a bioactive compound is added different behaviors can be found in literature: Ochnio et al. [12] observed an increase in the particle size of soybean 11S globulin after its interaction with folic acid. On the contrary, Penalva et al. [55] reported a drop in the aggregation of casein after its complexation with folic acid and Martinez et al. [11] did not observe changes in the particle size of the 11S globulin of quinoa when adding different concentrations of betanin.

The ζ-potential serves as a measure for the strength of electrostatic interactions among charges at the molecular surface level. Regarding to this, existing literature suggests that electrostatically stabilized hydrocolloids typically possess ζ-potentials surpassing absolute values of 40 mV, as observed by Andreeva et al. [56]. ζ -potentials obtained here for 11S-RSV and 11S-TOC nanocomplexes would not be high enough to keep the system stable. However, the systems remain colloidally stable. Thus, the physical stability does not seem to be rationally explained by electrostatic stabilization, suggesting other forces to dictate the systems stability[14]. A plausible explanation lies in steric overlap interactions, which maintain a separation distance for 11S-RSV and 11S-TOC nanocomplexes, thereby contributing to the stability of the system. These interactions also play a key role in influencing factors like particle size distribution, cellular uptake, and adsorption to cellular membranes in vivo, as highlighted by Fröhlich [57]. For comparison, it could be mentioned that Corfield et al. [8] and Relkin & Shukat [58] reported ζ-potentials of -23 and -42 mV for solutions of bovine whey protein isolates (WPI) and concentrates (WPC), respectively. These values of ζ-potential, especially that highest corresponding to WPC, would reflect a greater contribution of electrostatic interactions of complexes by the repulsion, increasing the physical stabilization of the dispersions. Corfield et al. [9] and Perez et al. [14] also detect changes in this parameter because of the addition of folic acid (FA) to dairy protein solutions.

Differences in sizes values obtained from DLS and AFM could be explained in terms of the relationships between sample mounting and the chemical nature of the material under examination. Tiwari et al. [59] attribute such differences to the surface accumulation of protein molecules during sample preparation as spreading and drying, which are very common phenomena. One must be in mind that samples visualized with AFM lack hydration layer which contribute to discrepancies in size. In our case, diameters of 35 and 45 nm were obtained for single 11S by DLS and AFM, respectively. Both types of nanocomplexes, 11S-RSV and 11S-TOC gave dimensions of 100 nm as measured by AFM. Meanwhile hydrodynamic diameters of 72 and 140 nm were registered by DLS for 11S-RSV and 11S-TOC nanocomplexes, respectively.

From nanocomplexes functional point of view, the non-decrease in the antioxidant capacity after their formation allowed the single components beneficial characteristic to be maintained after

 doi:10.20944/preprints202407.1087.v1

complexation as there are reports indicating that the additive effect in the antioxidant capacity may not be a generality, for example Rashidinejad et al.[60] observed a detriment to the antioxidant capacity of tea polyphenols after their complexation with dairy proteins.

With respect to mixed systems, the trend for 11S-TOC was similar as with ABTS: antioxidant activity of the complexes was due to the antioxidant capacity of the 11S globulin. Instead, the effect of combining 11S and RSV resulted additive. This additive effect implies that the antioxidant capacity of RSV was improved by its complexation with 11S globulin. The term "additive" was once employed to characterize composite systems that exhibited a higher value for a particular physicochemical property compared to the individual components and, in turn, the attained value did not surpass the sum of the individual components [61]. Based in these results, we attribute the mentioned additive character of the 11S-RSV complexes to the intrinsic antioxidant capacity of 11S globulin.

It is noteworthy, that the antioxidant effectiveness of a specific compound may differ across various methods due to factors like the reaction mechanism employed, solubility of the antioxidant, oxidation state, pH, and the nature of the substrate prone to oxidation. According to this Biskup et al. [62], who analyzed the antioxidant activity of phenols by both, FRAP and ABTS essays, found differences between both techniques. Therefore, its recommendable to investigate the antioxidant capacity through at least two methods [63].

Mixed systems constituted by 11S-RSV and 11S-TOC exhibited characteristics of ground-state complexes, suggesting their potential application as a delivery system. The obtained results contribute to considering the 11S as a feasible carrier agent for RSV and TOC vehicle and protection.

5. Conclusions

In this work, a strategy was developed to design and characterize complexes constituted by 11S quinoa seed globulin and RSV or TOC. Particle size distribution allow to conclude that these complexes suffered macromolecular aggregation induced after complexation. Such complexes/aggregates dimensions fell into the nanoscale, constituting nanocomplexes, which could serve as vehicles for the bioactive compound keeping its health beneficial effects in the presence of light, certain pH and enzymes, during food processing and path through gastrointestinal tract.

We demonstrated that TOC, the biologically active variant of lipophilic vitamin E, and RSV a natural polyphenol with antioxidant properties, bound to extracted and purified quinoa seed 11S globulin. Employing different approaches, it can be confirmed that RSV and TOC interacted with 11S in a stable way. Punctually, molecular docking, fluorescence analysis, and ITC were employed to gain insights into the molecular interactions between quinoa seed 11S globulin and RSV or TOC. These approaches allow us to obtain affinity constant values and to confirmed that the interaction between 11S globulin and RSV or TOC primarily involves non-covalent binding. In fact, it was seen that the interaction between 11S and RSV is stronger than that 11S and TOC. Mixed systems constituted by 11S-RSV and 11S-TOC exhibited characteristics of ground-state complexes, suggesting their potential application as a delivery system. The obtained results contribute to considering the 11S as a feasible carrier agent for RSV and TOC vehicle and protection. These nanocomplexes could constitute a real platform for the design of functional ingredients and nutraceutical products. This research line will continue with the investigation above the behavior of the biological performance of these nanocomplexes, i.e. antioxidant properties, bioaccessibility and bioavailability assessed in in-vitro systems.

Supplementary Materials: The following supporting information can be downloaded at the website of this paper posted on Preprints.org.

Author Contributions: Alejandra J. Rubinstein: Conceptualization, Formal analysis, Investigation, Validation, Visualization, Writing - original draft. **Guadalupe Garcia Liñares:** Resources, Supervision, Writing - review & editing. **Valeria Boeris:** Resources, Supervision, Writing - review & editing. **Oscar E. Pérez:** Conceptualization, Funding acquisition, Project administration, Resources, Supervision, Writing - review & editing.

Funding: This work was supported by the Universidad de Buenos Aires - UBA (UBACYT Nº 20020190100297BA); the Agencia Nacional de Promoción Científica y Tecnológica - ANPCyT (PICT 2021-0347)

and the Consejo Nacional de Investigaciones Científicas y Técnicas - CONICET (PIP 2022-2024 GI 11220210100072CO).

Institutional Review Board Statement: "Not applicable"

Informed Consent Statement: "Not applicable."

Data Availability Statement: Data will be made available on request.

Conflicts of Interest The authors declare no conflicts of interest.

References

1. He, X.; Wang, B.; Zhao, B.; Yang, F. Ultrasonic Assisted Extraction of Quinoa (Chenopodium Quinoa Willd.) Protein and Effect of Heat Treatment on Its In Vitro Digestion Characteristics. *Foods* **2022**, *11*, doi:10.3390/foods11050771.
2. Lingiardi, N.; Galante, M.; de Sanctis, M.; Spelzini, D. Are Quinoa Proteins a Promising Alternative to Be Applied in Plant-Based Emulsion Gel Formulation? *Food Chem* **2022**, *394*, doi:10.1016/j.foodchem.2022.133485.
3. Kaspchak, E.; Oliveira, M.A.S. de; Simas, F.F.; Franco, C.R.C.; Silveira, J.L.M.; Mafra, M.R.; Igarashi-Mafra, L. Determination of Heat-Set Gelation Capacity of a Quinoa Protein Isolate (Chenopodium Quinoa) by Dynamic Oscillatory Rheological Analysis. *Food Chem* **2017**, *232*, 263–271, doi:10.1016/j.foodchem.2017.04.014.
4. Choi, I.; Li, N.; Zhong, Q. Enhancing Bioaccessibility of Resveratrol by Loading in Natural Porous Starch Microparticles. *Int J Biol Macromol* **2022**, *194*, 982–992, doi:10.1016/j.ijbiomac.2021.11.157.
5. Chimento, A.; De Amicis, F.; Sirianni, R.; Sinicropi, M.S.; Puoci, F.; Casaburi, I.; Saturnino, C.; Pezzi, V. Progress to Improve Oral Bioavailability and Beneficial Effects of Resveratrol. *Int J Mol Sci* **2019**, *20*, doi:10.3390/ijms20061381.
6. Saini, R.K.; Keum, Y.S. Tocopherols and Tocotrienols in Plants and Their Products: A Review on Methods of Extraction, Chromatographic Separation, and Detection. *Food Research International* **2016**, *82*, 59–70, doi:10.1016/j.foodres.2016.01.025.
7. Bustos, L.F.; Judis, M.A.; Vasile, F.E.; Pérez, O.E. Molecular Interactions Involved in the Complexation Process between Buffalo Whey Proteins Concentrate and Folic Acid. *Food Chem* **2022**, *396*, doi:10.1016/j.foodchem.2022.133734.
8. Corfield, R.; Martínez, K.D.; Allievi, M.C.; Santagapita, P.; Mazzobre, F.; Schebor, C.; Pérez, O.E. Whey Proteins-Folic Acid Complexes: Formation, Isolation and Bioavailability in a Lactobacillus Casei Model. *Food Structure* **2020**, *26*, doi:10.1016/j.foostr.2020.100162.
9. Corfield, R.; Lalou, G.; Di Lella, S.; Martínez, K.D.; Schebor, C.; Allievi, M.C.; Pérez, O.E. Experimental and Modeling Approaches Applied to the Whey Proteins and Vitamin B9 Complexes Study. *Food Hydrocoll* **2023**, *142*, doi:10.1016/j.foodhyd.2023.108834.
10. Liu, K.; Zha, X.Q.; Li, Q.M.; Pan, L.H.; Luo, J.P. Hydrophobic Interaction and Hydrogen Bonding Driving the Self-Assembling of Quinoa Protein and Flavonoids. *Food Hydrocoll* **2021**, *118*, doi:10.1016/j.foodhyd.2021.106807.
11. Martínez, J.H.; Velázquez, F.; Burrieza, H.P.; Martínez, K.D.; Paula Domínguez Rubio, A.; dos Santos Ferreira, C.; del Pilar Buera, M.; Pérez, O.E. Betanin Loaded Nanocarriers Based on Quinoa Seed 11S Globulin. Impact on the Protein Structure and Antioxidant Activity. *Food Hydrocoll* **2019**, *87*, 880–890, doi:10.1016/j.foodhyd.2018.09.016.
12. Ochnio, M.E.; Martínez, J.H.; Allievi, M.C.; Palavecino, M.; Martínez, K.D.; Pérez, O.E. Proteins as Nano-Carriers for Bioactive Compounds. The Case of 7S and 11S Soy Globulins and Folic Acid Complexation. *Polymers (Basel)* **2018**, *10*, doi:10.3390/polym10020149.
13. Kiss Nanotechnology in Food Systems: A Review. *Acta Aliment* **2020**, *49*, 460–474, doi:10.1556/066.2020.49.4.12.
14. Pérez, O.E.; David-Birman, T.; Kesselman, E.; Levi-Tal, S.; Lesmes, U. Milk Protein-Vitamin Interactions: Formation of Beta-Lactoglobulin/Folic Acid Nano-Complexes and Their Impactoninvitro Gastro-Duodenal Proteolysis. *Food Hydrocoll* **2014**, *38*, 40–47, doi:10.1016/j.foodhyd.2013.11.010.
15. Laemmli Cleavage of Structural Proteins during the Assembly of the Head of bacteriophage T4. **1970**, doi:https://doi.org/10.1038/227680a0.
16. Neuhoff, V.; Arold, N.; Taube, D.; Ehrhardt, W. Improved Staining of Proteins in Polyacrylamide Gels Including Isoelectric Focusing Gels with Clear Background at Nanogram Sensitivity Using Coomassie Brilliant Blue G-250 and R-250. *Electrophoresis* **1988**, *9*, 255–262, doi:10.1002/elps.1150090603.
17. Trott, O.; Olson, A.J. AutoDock Vina: Improving the Speed and Accuracy of Docking with a New Scoring Function, Efficient Optimization, and Multithreading. *J Comput Chem* **2010**, *31*, 455–461, doi:10.1002/jcc.21334.

18. William Humphrey; Andrew Dalke; Klaus Schulten VMD: Visual Molecular Dynamics., doi:https://doi.org/10.1016/0263-7855(96)00018-5.
19. Liang, L.; Subirade, M. β-Lactoglobulin/Folic Acid Complexes: Formation, Characterization, and Biological Implication. *Journal of Physical Chemistry B* **2010**, *114*, 6707–6712, doi:10.1021/jp101096r.
20. Lakowicz, J.R.; Weber, G. Quenching of Fluorescence by Oxygen. a Probe for Structural Fluctuations in Macromolecules. *Biochemistry* **1973**, *12*, 4161–4170, doi:10.1021/bi00745a020.
21. Bian, Q.; Liu, J.; Tian, J.; Hu, Z. Binding of Genistein to Human Serum Albumin Demonstrated Using Tryptophan Fluorescence Quenching. *Int J Biol Macromol* **2004**, *34*, 275–279, doi:10.1016/j.ijbiomac.2004.09.005.
22. Wei, X.L.; Xiao, J.B.; Wang, Y.; Bai, Y. Which Model Based on Fluorescence Quenching Is Suitable to Study the Interaction between Trans-Resveratrol and BSA? *Spectrochim Acta A Mol Biomol Spectrosc* **2010**, *75*, 299–304, doi:10.1016/j.saa.2009.10.027.
23. Demirkaya, F.; Kadioglu, Y. Simple GC-FID Method Development and Validation for Determination of α-Tocopherol (Vitamin E) in Human Plasma. *J Biochem Biophys Methods* **2007**, *70*, 363–368, doi:10.1016/j.jbbm.2006.08.006.
24. Carpineti, L.; Martinez, M.J.; Pilosof, A.M.R.; Pérez, O.E. β-Lactoglobulin-Carboxymethylcellulose Core-Shell Microparticles: Construction, Characterization and Isolation. *J Food Eng* **2014**, *131*, 65–74, doi:10.1016/j.jfoodeng.2014.01.018.
25. Montserrat-de la Paz, S.; Rodriguez-Martin, N.M.; Villanueva, A.; Pedroche, J.; Cruz-Chamorro, I.; Millan, F.; Millan-Linares, M.C. Evaluation of Anti-Inflammatory and Atheroprotective Properties of Wheat Gluten Protein Hydrolysates in Primary Human Monocytes. *Foods* **2020**, *9*, doi:10.3390/foods9070854.
26. Rocha, G.F.; Kise, F.; Rosso, A.M.; Parisi, M.G. Potential Antioxidant Peptides Produced from Whey Hydrolysis with an Immobilized Aspartic Protease from Salpichroa Origanifolia Fruits. *Food Chem* **2017**, *237*, 350–355, doi:10.1016/j.foodchem.2017.05.112.
27. Ruiz, G.A.; Xiao, W.; Van Boekel, M.; Minor, M.; Stieger, M. Effect of Extraction PH on Heat-Induced Aggregation, Gelation and Microstructure of Protein Isolate from Quinoa (Chenopodium Quinoa Willd). *Food Chem* **2016**, *209*, 203–210, doi:10.1016/j.foodchem.2016.04.052.
28. Brinegar, C.; Goundan, S. Isolation and Characterization of Chenopodin, the 11S Seed Storage Protein of Quinoa (Chenopodium Quinoa). *J. Agrlc. FoodChem* **1993**, *1883*, 182–185, doi:https://doi.org/10.1021/jf00026a006.
29. Abugoch, L.E.; Martínez, N.E.; Añón, M.C. Influence of PH on Structure and Function of Amaranth (Amaranthus Hypochondriacus) Protein Isolates. *Cereal Chem* **2010**, *87*, 448–453, doi:10.1094/CCHEM-09-09-0125.
30. Shahraki, S.; Heydari, A.; Saeidifar, M.; Gomroki, M. Biophysical and Computational Comparison on the Binding Affinity of Three Important Nutrients to β-Lactoglobulin: Folic Acid, Ascorbic Acid and Vitamin K3. *J Biomol Struct Dyn* **2018**, *36*, 3651–3665, doi:10.1080/07391102.2017.1394222.
31. Maity, S.; Pal, S.; Sardar, S.; Sepay, N.; Parvej, H.; Chakraborty, J.; Chandra Halder, U. Multispectroscopic Analysis and Molecular Modeling to Investigate the Binding of Beta Lactoglobulin with Curcumin Derivatives. *RSC Adv* **2016**, *6*, 112175–112183, doi:10.1039/C6RA24275H.
32. Mantovani, R.; Hamon, P.; Rousseau, F.; Tavares, G.; Mercadante, A.Z.; Croguennec, T.; Bouhallab, S.; Zerlotti Mer-Cadante, A.; Mantovani, R.A.; Tavares, G.M.; et al. Unraveling the Molecular Mechanisms Underlying Interactions between Caseins and Lutein. *Food Research International* **2020**, *138*, 963–9969, doi:10.1016/j.foodres.2020.109781ï.
33. Zhao, Y.; Chen, F.; Gao, C.; Feng, X.; Tang, X. Structure, Physical and Antioxidant Properties of Quinoa Protein /Hsian-Tsao Gum Composite Biodegradable Active Films. *LWT* **2022**, *155*, doi:10.1016/j.lwt.2021.112985.
34. Chilom, C.G.; Bacalum, M.; Stanescu, M.M.; Florescu, M. Insight into the Interaction of Human Serum Albumin with Folic Acid: A Biophysical Study. *Spectrochim Acta A Mol Biomol Spectrosc* **2018**, *204*, 648–656, doi:10.1016/j.saa.2018.06.093.
35. Gentile, L. Protein–Polysaccharide Interactions and Aggregates in Food Formulations. *Curr Opin Colloid Interface Sci* **2020**, *48*, 18–27, doi:10.1016/j.cocis.2020.03.002.
36. Chandel, T.I.; Zaman, M.; Khan, M.V.; Ali, M.; Rabbani, G.; Ishtikhar, M.; Khan, R.H. A Mechanistic Insight into Protein-Ligand Interaction, Folding, Misfolding, Aggregation and Inhibition of Protein Aggregates: An Overview. *Int J Biol Macromol* **2018**, *106*, 1115–1129, doi:10.1016/j.ijbiomac.2017.07.185.
37. Shimoni, E. Using AFM to Explore Food Nanostructure. *Curr Opin Colloid Interface Sci* **2008**, *13*, 368–374, doi:10.1016/j.cocis.2008.02.005.
38. Cao, H.; Sun, R.; Shi, J.; Li, M.; Guan, X.; Liu, J.; Huang, K.; Zhang, Y. Effect of Ultrasonic on the Structure and Quality Characteristics of Quinoa Protein Oxidation Aggregates. *Ultrason Sonochem* **2021**, *77*, doi:10.1016/j.ultsonch.2021.105685.

39. Orsini Delgado, M.C.; Nardo, A.; Pavlovic, M.; Rogniaux, H.; Añón, M.C.; Tironi, V.A. Identification and Characterization of Antioxidant Peptides Obtained by Gastrointestinal Digestion of Amaranth Proteins. *Food Chem* **2016**, *197*, 1160–1167, doi:10.1016/j.foodchem.2015.11.092.
40. Gülçin, I. Antioxidant Properties of Resveratrol: A Structure-Activity Insight. *Innovative Food Science and Emerging Technologies* **2010**, *11*, 210–218, doi:10.1016/j.ifset.2009.07.002.
41. Escribano, J.; Cabanes, J.; Jiménez-Atiénzar, M.; Ibañez-Tremolada, M.; Gómez-Pando, L.R.; García-Carmona, F.; Gandía-Herrero, F. Characterization of Betalains, Saponins and Antioxidant Power in Differently Colored Quinoa (Chenopodium Quinoa) Varieties. *Food Chem* **2017**, *234*, 285–294, doi:10.1016/j.foodchem.2017.04.187.
42. Zhang, X.; Wang, C.; Qi, Z.; Zhao, R.; Wang, C.; Zhang, T. Pea Protein Based Nanocarriers for Lipophilic Polyphenols: Spectroscopic Analysis, Characterization, Chemical Stability, Antioxidant and Molecular Docking. *Food Research International* **2022**, *160*, doi:10.1016/j.foodres.2022.111713.
43. Chamizo-González, F.; Heredia, F.J.; Rodríguez-Pulido, F.J.; González-Miret, M.L.; Gordillo, B. Proteomic and Computational Characterisation of 11S Globulins from Grape Seed Flour By-Product and Its Interaction with Malvidin 3-Glucoside by Molecular Docking. *Food Chem* **2022**, *386*, doi:10.1016/j.foodchem.2022.132842.
44. Patnode, K.; Demchuk, Z.; Johnson, S.; Voronov, A.; Rasulev, B. Computational Protein-Ligand Docking and Experimental Study of Bioplastic Films from Soybean Protein, Zein, and Natural Modifiers. *ACS Sustain Chem Eng* **2021**, *9*, 10740–10748, doi:10.1021/acssuschemeng.1c01202.
45. Chen, S.; Han, Y.; Huang, J.; Dai, L.; Du, J.; McClements, D.J.; Mao, L.; Liu, J.; Gao, Y. Fabrication and Characterization of Layer-by-Layer Composite Nanoparticles Based on Zein and Hyaluronic Acid for Codelivery of Curcumin and Quercetagetin. *ACS Appl Mater Interfaces* **2019**, *11*, 16922–16933, doi:10.1021/acsami.9b02529.
46. Ferina, J.; Daggett, V. Visualizing Protein Folding and Unfolding. *J Mol Biol* **2019**, *431*, 1540–1564, doi:10.1016/j.jmb.2019.02.026.
47. Li, X.; Ni, T. Probing the Binding Mechanisms of α-Tocopherol to Trypsin and Pepsin Using Isothermal Titration Calorimetry, Spectroscopic, and Molecular Modeling Methods. *J Biol Phys* **2016**, *42*, 415–434, doi:10.1007/s10867-016-9415-6.
48. Wan, Z.L.; Wang, L.Y.; Wang, J.M.; Yuan, Y.; Yang, X.Q. Synergistic Foaming and Surface Properties of a Weakly Interacting Mixture of Soy Glycinin and Biosurfactant Stevioside. *J Agric Food Chem* **2014**, *62*, 6834–6843, doi:10.1021/jf502027u.
49. Yang, T.; Yang, H.; Fan, Y.; Li, B.; Hou, H. Interactions of Quercetin, Curcumin, Epigallocatechin Gallate and Folic Acid with Gelatin. *Int J Biol Macromol* **2018**, *118*, 124–131, doi:10.1016/j.ijbiomac.2018.06.058.
50. Jiang, X.Y.; Li, W.X.; Cao, H. Study of the Interaction between Trans-Resveratrol and BSA by the Multi-Spectroscopic Method. *J Solution Chem* **2008**, *37*, 1609–1623, doi:10.1007/s10953-008-9323-x.
51. Li, W.; Bi, D.; Yi, J.; Yao, L.; Cao, J.; Yang, P.; Li, M.; Wu, Y.; Xu, H.; Hu, Z.; et al. Soy Protein Isolate-Polyguluronate Nanoparticles Loaded with Resveratrol for Effective Treatment of Colitis. *Food Chem* **2023**, *410*, doi:10.1016/j.foodchem.2023.135418.
52. Khan, M.A.; Fang, Z.; Wusigale; Cheng, H.; Gao, Y.; Deng, Z.; Liang, L. Encapsulation and Protection of Resveratrol in Kafirin and Milk Protein Nanoparticles. *Int J Food Sci Technol* **2019**, *54*, 2998–3007, doi:10.1111/ijfs.14212.
53. Carpentier, J.; Conforto, E.; Chaigneau, C.; Vendeville, J.E.; Maugard, T. Microencapsulation and Controlled Release of α-Tocopherol by Complex Coacervation between Pea Protein and Tragacanth Gum: A Comparative Study with Arabic and Tara Gums. *Innovative Food Science and Emerging Technologies* **2022**, *77*, doi:10.1016/j.ifset.2022.102951.
54. Xu, W.; Lv, K.; Mu, W.; Zhou, S.; Yang, Y. Encapsulation of α-Tocopherol in Whey Protein Isolate/Chitosan Particles Using Oil-in-Water Emulsion with Optimal Stability and Bioaccessibility. *LWT* **2021**, *148*, doi:10.1016/j.lwt.2021.111724.
55. Penalva, R.; Esparza, I.; Agüeros, M.; Gonzalez-Navarro, C.J.; Gonzalez-Ferrero, C.; Irache, J.M. Casein Nanoparticles as Carriers for the Oral Delivery of Folic Acid. *Food Hydrocoll* **2015**, *44*, 399–406, doi:10.1016/j.foodhyd.2014.10.004.
56. Andreeva, Y.I.; Drozdov, A.S.; Fakhardo, A.F.; Cheplagin, N.A.; Shtil, A.A.; Vinogradov, V. V. The Controllable Destabilization Route for Synthesis of Low Cytotoxic Magnetic Nanospheres with Photonic Response. *Sci Rep* **2017**, *7*, doi:10.1038/s41598-017-11673-4.
57. Fröhlich, E. The Role of Surface Charge in Cellular Uptake and Cytotoxicity of Medical Nanoparticles. *Int J Nanomedicine* **2012**, *7*, 5577–5591, doi:10.2147/IJN.S36111.
58. Relkin, P.; Shukat, R. Food Protein Aggregates as Vitamin-Matrix Carriers: Impact of Processing Conditions. *Food Chem* **2012**, *134*, 2141–2148, doi:10.1016/j.foodchem.2012.04.020.
59. Tiwari, K.; Singh, G.; Singh, S.K. Purification and Structural Characterization of N-Terminal 190 Amino Acid Deleted Essential Mammalian Protein; Transcription Termination Factor 1. *ACS Omega* **2022**, *7*, 45165–45173, doi:10.1021/acsomega.2c05603.

60. Rashidinejad, A.; Birch, E.J.; Sun-Waterhouse D.; Everett, D.W. Addition of Milk to Tea Infusions_ Helpful or Harmful_ Evidence from in Vitro and in Vivo Studies on Antioxidant Properties. **2017**, doi:10.1080/10408398.2015.1099515.
61. Pérez, O.E.; Carrera-Sánchez, C.; Rodríguez-Patino, J.M.; Pilosof, A.M.R. Adsorption Dynamics and Surface Activity at Equilibrium of Whey Proteins and Hydroxypropyl-Methyl-Cellulose Mixtures at the Air-Water Interface. *Food Hydrocoll* **2007**, *21*, 794–803, doi:10.1016/j.foodhyd.2006.11.013.
62. Izabela Biskup; Iwona Golonka; Andrzej Gamian; Zbigniew Sroka Antioxidant Activity of Selected Phenols Estimated by ABTS and FRAP Methods. **2013**, 958–963, doi:10.5604/17322693.1066062.
63. Schlesier, K.; Harwat, M.; Böhm, V.; Bitsch, R. Assessment of Antioxidant Activity by Using Different in Vitro Methods. *Free Radic Res* **2002**, *36*, 177–187, doi:10.1080/10715760290006411.